Tolerance to PVY infection in potato is conditioned by perturbation of small RNA– gibberellin regulatory network

Maja Križnik[1,2], Marko Petek[1], David Dobnik[1], Živa Ramšak[1], Špela Baebler[1], Stephan Pollmann[3], Jan Kreuze[4], Jana Žel[1], Kristina Gruden[1]

[1]Department of Biotechnology and Systems Biology, National Institute of Biology, Ljubljana, Slovenia

[2]Jožef Stefan International Postgraduate School, Ljubljana, Slovenia

[3]Centro de Biotecnología y Genómica de Plantas, Universidad Politécnica de Madrid (UPM) - Instituto Nacional de Investigación y Tecnología Agraria y Alimentaria (INIA), Campus de Montegancedo UPM, Madrid, Spain.

[4]Global Program of Integrated Crop and Systems Research, International Potato Center (CIP), Lima, Peru

* Corresponding author
E-mail: maja.kriznik@nib.si

Abstract

Potato virus Y (PVY) is the most economically important potato viral pathogen worldwide. We aimed at unraveling the roles of small RNAs (sRNAs) in the complex immune signaling network controlling the establishment of tolerant response of potato cv. Désirée to the virus. We identified and quantified the endogenous miRNAs and phasiRNAs as well as virus-derived sRNAs. We constructed a sRNA regulatory network connecting sRNAs and their targets identified to link sRNA level responses to physiological processes. We discovered an interesting novel sRNAs – gibberellin (GA) regulatory circuit being activated as early as 3 days post inoculation, before viral multiplication can be detected. Increased levels of miR167 and phasiRNA931 were reflected in decreased levels of transcripts involved in GA biosynthesis. Moreover, decreased concentration of GA confirmed this regulation. We have additionally showed that this regulation is salicylic acid dependent as the response of sRNA network was attenuated in salicylic acid-depleted transgenic counterpart NahG-Désirée expressing severe disease symptoms. Moreover, we found that differentially expressed miR6022, which targets leucine-rich-repeat

receptor-like kinases, likely links GA signaling with immune responses. Besides downregulation of GA signaling, regulation of several other parts of sRNA network in tolerant Désirée revealed striking similarities to responses observed in mutualistic symbiotic interactions. The intertwining of different regulatory networks revealed here shows how developmental signaling, symptomology and stress signaling are balanced.

Introduction

Potato (*Solanum tuberosum* L.) is the world's most important non-grain staple crop. Viruses pose a serious threat to potato production, not only because of the effects caused by the primary infection, but also because potato is propagated vegetatively so that viruses are transmitted through the tubers and accumulate over time [1]. The most devastating potato virus is *Potato virus Y* (PVY) [2]. PVY is a member of the Potyviridae family and comprises of many diverse strains. Worldwide, the most harmful strain is PVY^{NTN} which has been responsible for huge decreases in quality and quantity of potato tuber production [3]. One of the most widely grown potato cultivars is cv. Désirée, which is tolerant to PVY^{NTN}, meaning that the virus replicates and spreads systemically, however, symptoms of the disease are reduced or not visible at all [4,5]. Tolerance may have an advantage over resistance for crop protection because it does not actively select against virus infection and replication, therefore there is little evolutionary pressure for PVY to mutate. Hence, the tolerant phenotype is likely to be more durable than resistance [6]. Until now, studies on Désirée-PVY^{NTN} interactions have focused on the detection of changes in the plant transcriptome and proteome, particularly those related to plant hormonal signaling [5,7]. Salicylic acid (SA) was found to be the crucial component for attenuation of the disease symptoms [5]. However, understanding of the mechanisms that underlie tolerance response to PVY^{NTN} is still incomplete.

RNA silencing is a basal antiviral system in plants, where DICER-like proteins cleave viral dsRNA structures, giving rise to virus-derived small interfering RNAs (vsiRNAs), which are then incorporated into Argonaute (AGO) protein(s) to guide viral RNA degradation [8]. To counter this host defense mechanism, viruses have evolved viral suppressors of RNA silencing [9]. Helper component-proteinase (HC-Pro) of potyviruses suppresses silencing by sequestering small RNAs (sRNAs) and AGO1 and thus counteracts the degradation of viral RNA [10]. Another level of plant antiviral defense is mediated by resistance genes, leading towards effector triggered immunity, often resulting in hypersensitive response and programmed cell death [11]. The cv. Désirée carries the *Ny* gene conferring resistance against strain PVY^{O}, but lacks resistance genes against the PVY^{NTN} strain [12] and thus does not respond by triggering an efficient effector triggered immunity.

Recent findings revealed that endogenous RNA silencing mediated by microRNAs (miRNAs) and small interfering RNAs (siRNAs) could play important roles in plant immunity [13]. These 18-24-nt long non-coding sRNAs are able to negatively regulate gene expression by binding to the specific mRNA targets which leads to either promoting their degradation, inhibiting their translation, or suppressing transcription by epigenetic modification [8,14]. The endogenous RNA silencing can be amplified by the production of secondary phased siRNAs (phasiRNAs), triggered by 22-nt miRNAs/siRNAs [15,16]. phasiRNAs are generated in phase relative to positions of the miRNA cleavage site, can be produced from both coding and non-coding transcript (*PHAS* loci) and are able to target transcripts not only in *trans* but also their *PHAS* loci of origin in *cis* and thus additionally contribute to the autoregulation [17]. miRNAs have been associated with defense responses against several pathogens [18]. Arabidopsis miR393 was the first plant miRNA reported to play a key role in antibacterial immunity by repressing auxin signaling [19]. Recently, several studies have uncovered the miRNA-mediated silencing of immune receptor gene (*R*-gene) transcripts. Infection by pathogens e.g. viruses or bacteria, relieves the silencing, leading to the accumulation of *R* proteins and activation of immune responses [20–22].

This growing body of evidence suggests that sRNAs are integral components of plant immunity. However, none of the studies performed so far investigated the sRNA regulatory network in potato – virus interaction at the systems level linking it to transcriptional regulation. The aim of this study was to investigate sRNAs' role in establishment of the tolerant response of potato to PVY^{NTN}, hence we have studied response in the early stage of viral infection, before the viral multiplication can be detected. Employing high-throughput sequencing technology, we characterized and compared the sRNA expression patterns between PVY-infected and healthy tolerant potato plants. In addition, this information was linked with expression profiles of their target transcripts identified by *in silico* and Degradome-Seq and used for sRNA regulatory network construction. Besides the already described regulation of *R*-gene transcripts we have discovered a previously undescribed connection between sRNAs and gibberellin (GA) biosynthesis representing an important link between defensive and developmental signaling pathways which was confirmed by hormonal content measurements. Additionally we showed that response of the discovered sRNA network was attenuated in susceptible, SA deficient NahG-Désirée, confirming the crucial role of SA in mediating responses leading towards establishment of the tolerance against PVY infection.

Results

Novel endogenous sRNAs identified in potato leaves

We identified 245 different previously described miRNAs (including 38 miRNA variants; isomiRs), belonging to 95 miRNA families in control and PVY^{NTN}-infected leaves of cv. Désirée using sRNA-Seq (**S1 Fig, S1 Dataset**). In addition, 141 novel miRNAs were detected, of those 12 were coded by multiple *MIR* loci. Novel miRNA sequences were assigned to 123 novel miRNA families (**S1 and S2 Datasets**).

When assessing the miRNA regulatory network, the amplification of silencing through phasiRNA biogenesis was also considered. In total, more than 4000 *PHAS* loci were predicted, coding for 2558 phasiRNAs. 124 loci were located on protein-coding regions of genes, with the majority encoding NBS-LRRs (nucleotide binding site-leucine rich repeat proteins) and LRR-RLKs (leucine rich repeat-receptor-like kinases) (**S3 and S4 Datasets**). Interestingly, several novel *PHAS* loci were discovered in coding regions of genes associated with stress signaling, such as *HSP70*, superoxide dismutase and auxin signaling F-box proteins (see **S1 Table** for the full list of genes used in this study together with their descriptions and corresponding IDs). We also confirmed that *StAGO1* is a *PHAS* locus, as previously described in Arabidopsis [23] (**S3 Dataset**).

We further compared miRNA expression profiles of PVY^{NTN}-infected versus mock inoculated leaves in early stages of virus infection (3 dpi, 1 day before detectable viral multiplication; [5,7]). In total, 57 unique miRNAs were found to be significantly differentially expressed in early stages of PVY^{NTN} infection (3 dpi) of Désirée plants. Virus infection predominantly caused an increase in miRNAs levels (**Fig 1, S1 Dataset**). Additionally, we identified 35 phasiRNAs as differentially regulated 3 dpi, mainly originating from noncoding *PHAS* and *NBS-LRR* loci (**Fig 1, S4 Dataset**).

To validate the obtained sRNA-Seq results, abundance of six differentially expressed miRNAs was analyzed by stem-loop RT-qPCR. As shown in **S2 Fig,** all sRNA-Seq differential expression results were confirmed.

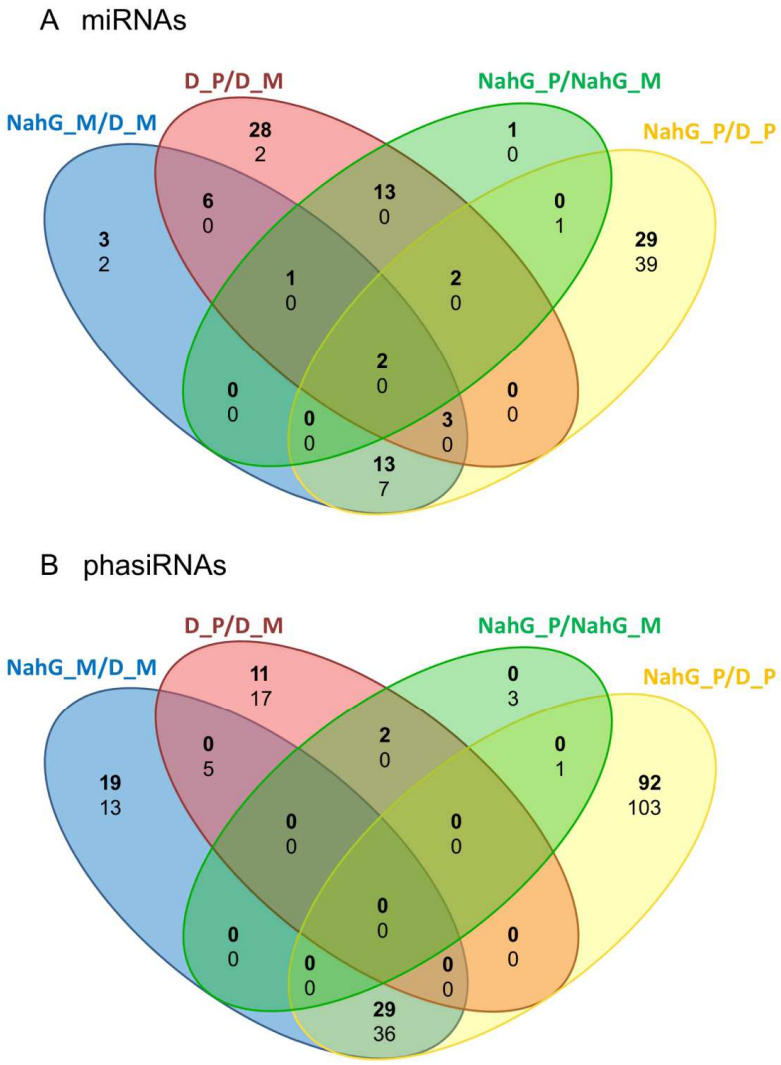

Fig 1. Numbers of unique and common differentially expressed miRNAs and phasiRNAs 3 days post PVY^{NTN} inoculation. Venn diagrams show the number of differentially expressed (FDR corrected p-value < 0.05) (**A**) miRNAs and (**B**) phasiRNAs in mock- or PVY^{NTN}-inoculated potato leaves of cv. Désirée and NahG-Désirée. Upregulated miRNAs/phasiRNAs are shown in bold and downregulated in normal text. D – Désirée, NahG – NahG-Désirée, M – mock, P – PVY^{NTN}.

In previous studies, a plethora of potato miRNA/phasiRNAs have been shown to be differentially expressed following pathogen infection. However, the biological relevance of these differences remains largely unknown. To translate the data obtained on sRNA level into changes in physiological processes, we performed *in silico* sRNA target prediction, both at the levels of translational inhibition and target cleavage (**S5 Dataset**). Additionally, the predictions of target cleavage were experimentally validated by Degradome-Seq (**S6 Dataset**). Based on this information we constructed a potato sRNA regulatory network connecting miRNAs with phasiRNAs and their targets (**Supplemental Online Files 1 and 2**). This revealed several already known and many novel connections related to the plant immune signaling (see example in **S3 Fig; S5 and S6 Datasets**). Interesting targets of differentially expressed miRNAs

and phasiRNAs encode defense related proteins such as pathogenesis-related (PR) proteins and proteins involved in the biosynthesis of secondary metabolites, transcription factors belonging to AP2/ERF, bHLH, MYB and GRAS family proteins, putative immune receptors (NBS-LRRs, LRR-RLKs) as well as proteins involved in biosynthesis and signaling of different phytohormones (**Fig 2**).

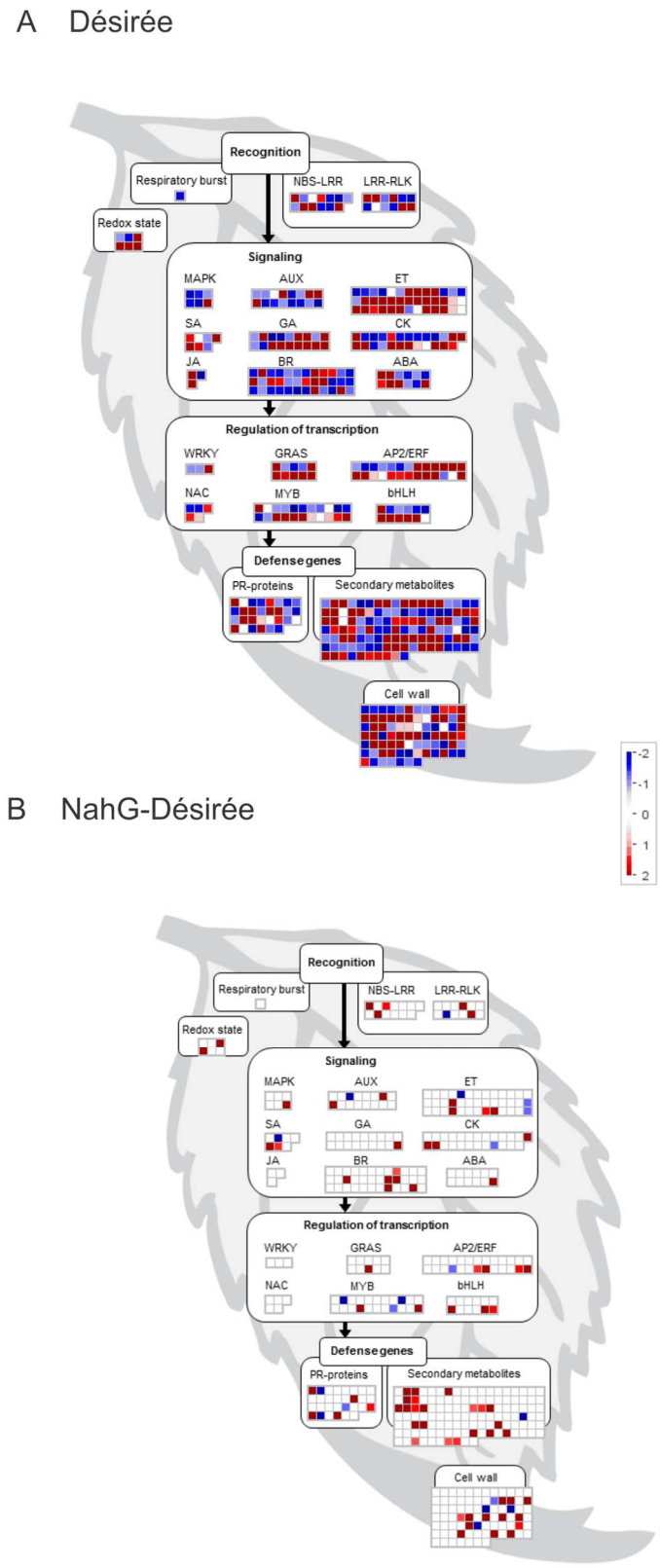

Fig 2. PVY induced changes in sRNA regulatory network at the onset of viral multiplication are controlling multiple immune signaling components. Visualization of differentially expressed miRNAs/phasiRNAs in (**A**) Désirée and (**B**) NahG-Désirée plants according to the function of their targets. Each square represents $\log_2$ ratios of expression between PVY^{NTN}- and mock-inoculated plants (red – upregulated; blue – downregulated). MapMan ontology bins: respiratory burst (20.1.1), redox state (21.6), MAPK (30.6), SA (17.8), JA (17.7), AUX (17.2), GA (17.6), BR (17.3), ET (17.5), CK (17.4), ABA (17.1), WRKY (27.3.32), NAC (27.3.27), GRAS (27.3.21), MYB (27.3.25), AP2/ERF (27.3.3), bHLH (27.3.6), PR-proteins (20.1.7), secondary metabolites (16), cell wall (10). The NBS-LRR and LRR-RLK bins were custom constructed for this study, based on their harboring domains (obtained from PFAM database; [24]). These bins represent differentially expressed miRNAs/phasiRNAs targeting NBS-LRRs or LRR-RLKs. NBS-LRR – nucleotide binding site-leucine-rich repeat protein, LRR-RLK – leucine-rich repeat receptor-like kinase, MAPK – mitogen activated protein kinase, SA – salicylic acid, JA – jasmonic acid, AUX – auxin, GA – gibberellin, BR – brassinosteroid, ET – ethylene, CK – cytokinin, ABA – abscisic acid, PR – pathogenesis-related.

Several miRNA-mRNA pairs conserved across plant species, such as miR156-*SPL11*, miR160-*ARF10*, miR172-*AP2* or miR396-*GRF5* [25], were confirmed also in our system (**S5 and S6 Datasets**). Our data also showed the miR393-mediated cleavage of transcripts encoding members of *TIR/AFB* gene family, receptors implicated in the control of auxin signaling (**Fig 3**). We also discovered that these transcripts were targets of several *TIR1*-derived phasiRNAs (phasiTIRs) (**Fig 3, S5 and S6 Datasets**). Moreover, we identified that the miR393- and phasiTIR-network is also targeting downstream transcription factor StARF1 and other phytohormone signaling pathways, such as transcripts involved in ethylene signaling (*StERF2a, StAP2,* and *StEIN4*), in jasmonate signaling (*StLOX1* and *StOPR1*) and in brassinosteroid biosynthesis (*StDWF4*) (**Fig 3, S5 and S6 Datasets**) indicating much larger complexity of sRNA network regulation as so far predicted.

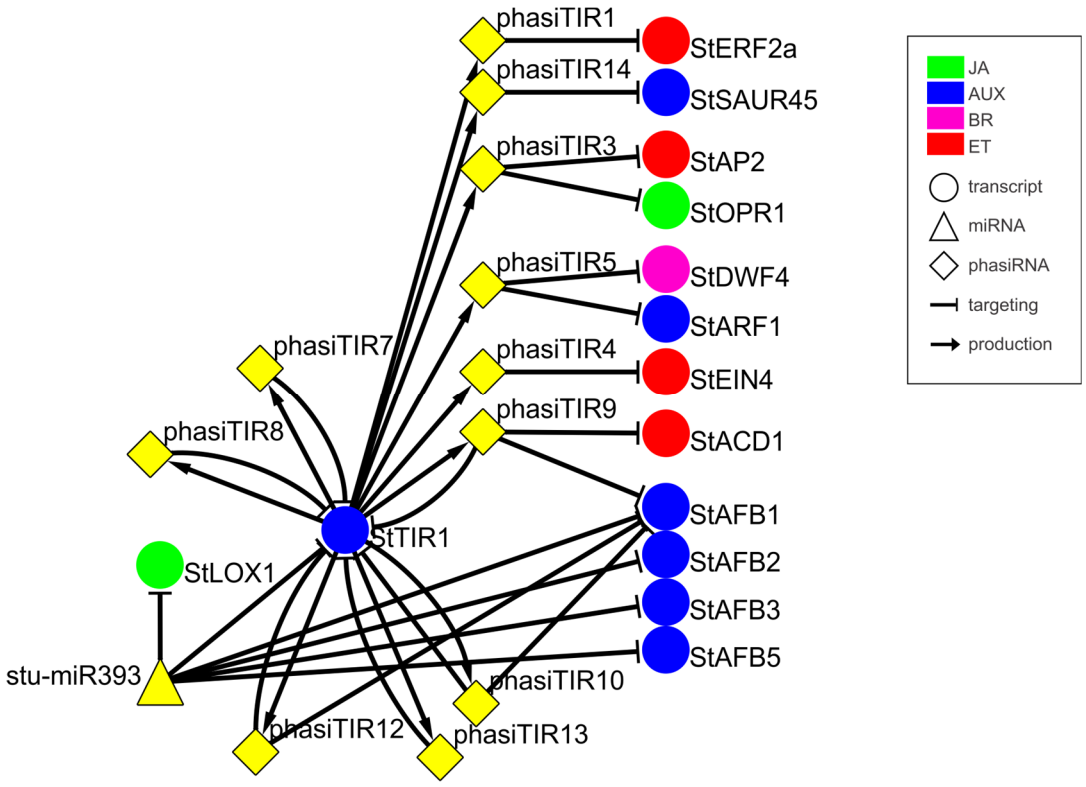

Fig 3. **miR393-mediated cleavage of StTIR1 leads to production of phasiTIRs targeting diverse phytohormone signaling components**. Node shapes represent classes of sRNAs (triangle – miRNA; diamond – phasiRNA) or transcripts (circle). Node colors indicate components related to different hormone signaling pathways: green – jasmonic acid (JA); blue – auxin (AUX); magenta – brassinosteroid (BR); red – ethylene (ET). Arrows connect sRNAs and targets (blunt-end arrow) or *PHAS* loci and producing phasiRNAs (regular arrow). Node stu-miR393 represents miR393-5p and miR393-5p.1 and node StAFB1 represents StAFB1.1, StAFB1.2, and StAFB1.3. For details of the target transcripts/genes see **Supplementary File 6**. StTIR1 – Transport inhibitor response 1, StLOX1 – Lipoxygenase 1, StERF2a – Ethylene responsive transcription factor 2a, StSAUR45 – Small auxin upregulated RNA 45, StAP2 – APETALA2, StOPR1 – 12-oxophytodienoate (OPDA) reductase, StDWF4 – Dwarf4, StARF1 – Auxin response factor 1, StEIN4 – Ethylene insensitive 4, StACD1 – 1-aminocyclopropane-1-carboxylic acid deaminase 1, StAFB1/2/3/5 – Auxin F-box 1/2/3/5.

Differentially expressed miRNAs regulate various immune receptor genes in tolerant response

Analysis of the differentially expressed miRNAs and phasiRNAs together with the levels of the target transcripts (data published in [7]) revealed the presence of many known, as well as novel, regulatory cascades involving *NBS-LRR*s. Several *NBS-LRR*s were predicted to be targeted by miR482, miR6024 and miR6027 family members (**S5 and S6 Datasets**). Moreover, *NBS-LRRs* are regulated also by phasiRNAs, where most phasiRNAs have multiple *NBS-LRR* targets (**S4 Fig**, **S5 and S6 Datasets**) due to the shared conserved P-loop or Walker A motif [21]. In all of the previous studies miR482 family members were downregulated following pathogen infection [21,26,27]. In our study, however, the one regulated member of the miR482 family (miR482e-5p) targeting *NBS-LRR* transcripts was upregulated following PVY^{NTN} infection (**S1 Dataset**), similarly as observed in establishment of mutualistic symbiosis in soybean roots [28]. Moreover, several miRNAs that were upregulated in response to PVY^{NTN} in cv. Désirée, such as miR164, miR167, miR171, miR319, miR390, miR393, miR397 and miR398 have also been reported to regulate nodulation in different legume species (**S1 Dataset**; [29–32]. In addition to NBS-LRR proteins, LRR-RLKs are also important mediators of immune signaling cascades. We have identified a novel miRNA-LRR-RLK interaction in which miR6022 levels decrease in response to PVY^{NTN} infection in cv. Désirée, which is further linked to upregulation of its predicted target genes encoding LRR-RLKs (**S4A Fig**).

Several PVY^{NTN}- derived siRNAs trigger degradation of host transcripts

The primary plant defense mechanism against invading viruses is RNA silencing involving the production of vsiRNAs. The population of vsiRNAs detected in the infected samples consisted of more than 46 000 unique sequences of 20-24 nt in length (**S7 Dataset**). In order to take into account the unlikely possibility that PVY^{NTN} produces its own miRNAs, we first ran the miRNA prediction pipeline on vsiRNAs and the viral genome. However, we found no sequence that would fullfill the criteria for a viral miRNA. Subsequently, we searched for potential host transcripts targeted by vsiRNAs in our experimentally validated target degradation dataset (**S8 Dataset**). We found that vsiRNAs are indeed

able to target multiple potato transcripts, among them mRNAs coding for immune receptor proteins, various transcription factors and proteins involved in hormonal signaling pathways (**S8 Dataset**). For example, several vsiRNAs were detected with the confirmed ability to guide the cleavage of transcripts involved in auxin signaling, transcripts encoding IAA-amino acid hydrolases (StILR1 and StIAR3), Aux/IAA transcriptional repressors (StIAAs) and the transcription factor StARF2.

sRNA-mediated downregulation of GA biosynthesis genes is reflected in lower GA_3 levels

Interestingly, we found that GA biosynthesis and downstream signaling are targeted by a sRNA-mediated regulatory network and that the changes in sRNA levels following PVY^{NTN} infection are reflected also in the changes of their target transcripts levels (**Fig 4A, S5 Dataset**). GA20-oxidase (GA20ox) and GA3-oxidase (GA3ox) are enzymes that catalyze the last steps in the formation of bioactive GAs [33]. We found that in Désirée plants the *StGA20ox* transcript is regulated by miR167e-3p (**Fig 4A**). An additional layer of GA biosynthesis regulation is represented by increased production of phasiRNA931, which promotes cleavage of the *StGA3ox* transcript. The transcriptomics results support these interactions as the targeted transcripts are significantly downregulated in Désirée upon PVY^{NTN} infection (**Fig 4A, S5 Dataset**). Additionally, vsiRNAs were found to target transcripts encoding two enzymes involved in GA biosynthesis *StGA1 and StGA20ox* (**Fig 4A, S8 Dataset**). One also has to note that all of the miRNAs/phasiRNAs discovered to be involved in sRNA-GA biosynthesis regulation have so far not been identified in Arabidopsis and among them only miR167 was also discovered in tomato [34,35].

Downstream GA signaling is also targeted by sRNAs in the potato – PVY interaction on multiple levels. The four miR319 family members were predicted to cleave the transcript encoding StMYB33, a GAMYB-like transcription factor orthologue [36], whereas phasiRNA931 targets a potato orthologue of a DELLA protein, a GA-signaling repressor (**Fig 4A**).

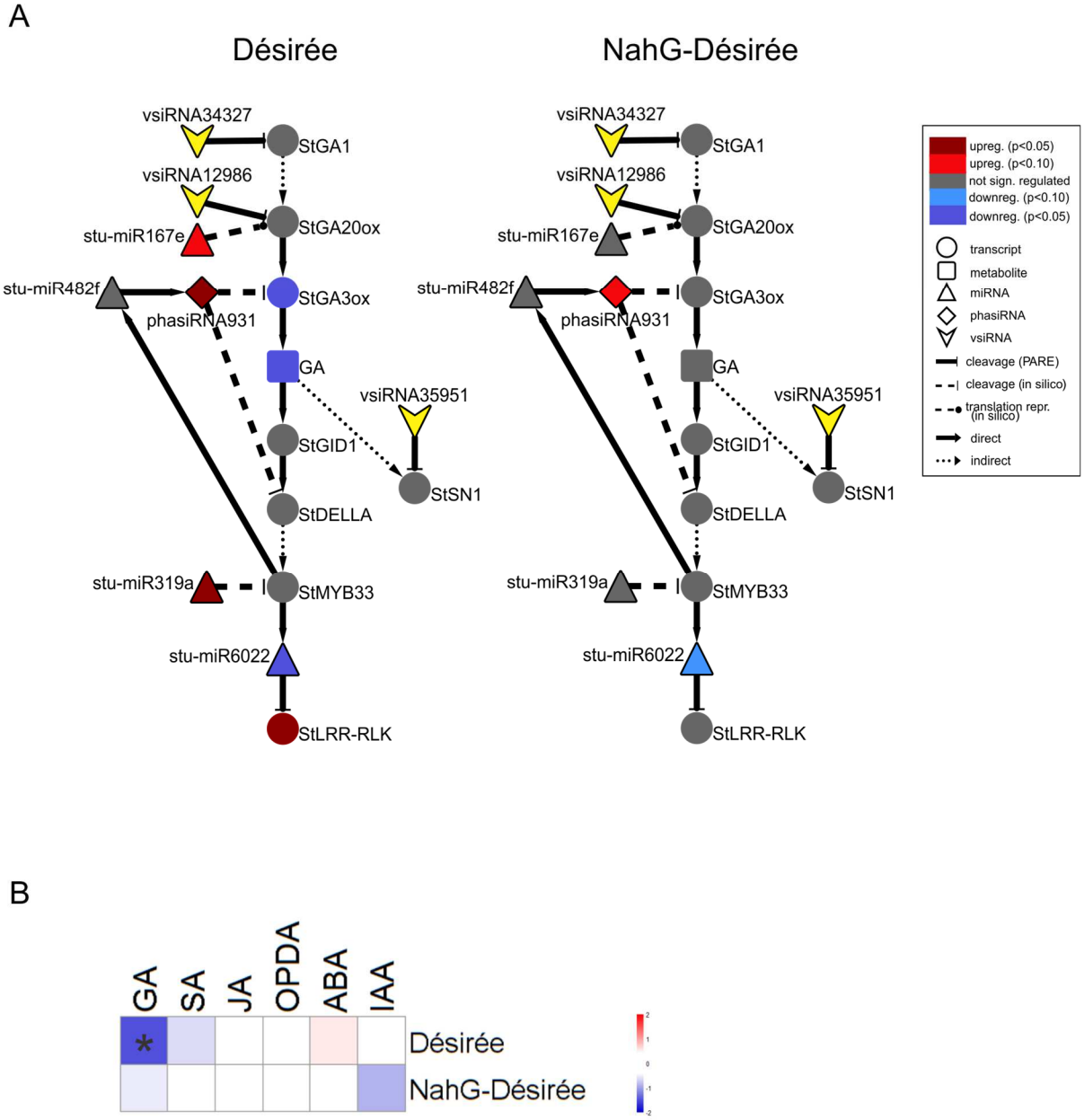

Fig 4. **miRNAs/phasiRNAs negatively regulate gibberellin (GA) biosynthesis and signaling.** (**A**) Networks of endogenous sRNAs and vsiRNAs targeting mRNAs of GA biosynthesis and signaling pathways in Désirée and NahG-Désirée plants 3 days post PVY^{NTN} inoculation. Node shape represent classes of sRNAs (triangle – miRNA; diamond – phasiRNA; arrowhead – vsiRNA), transcripts (circle) or metabolites (rectangle). Statistical significances of expression differences (p-values) and direction of expression change are represented by the node colors (see the legend). Arrows indicate type of interaction (solid-line normal arrow – direct interaction; dashed-line normal arrow – indirect interaction; blunt-end solid arrow – cleavage observed by Degradome-Seq, blunt-end dashed-line arrow – in silico predicted cleavage (or translational repression as proposed in [37]), dashed-line oval arrow – *in silico* predicted translational repression). Node stu-miR319a represents stu-miR319a-3p, stu-miR319a-3p.2, stu-miR319a-3p.4 and stu-miR319b-3p. Node StGA20ox represents StGA20ox, StGA20ox1, StGA20ox3 and StGA20ox4. For details of the target transcripts/genes see **S1 Table**. Stu-miR167e – stu-miR167e-3p; stu-miR482f – miR482f-3p; stu-miR6022 – miR6022-3p; StGA1 – GA REQUIRING 1 (ent-copalyl diphosphate synthase); StGA20ox – GA20-oxidase; StGA3ox – GA3-oxidase; StGID1C – GA receptor - GA INSENSITIVE DWARF1C hydrolase; StSN1 – Snakin-1; StDELLA – DELLA protein; StLRR-RLK – leucine-rich repeat receptor-like protein kinase. (**B**) Changes in concentrations of a set of plants hormones in Désirée and NahG-Désirée plants 3 days after PVY^{NTN} infection. sRNA-mediated repression of GA biosynthesis was confirmed by reduced GA_3 levels in PVY-infected Désirée plants**.** Colors present as log_2 ratios of mean concentrations between

PVY^{NTN}- and mock-inoculated plants (n=4; red – increased, blue – decreased level). * - indicate statistically significant values (ANOVA; $p < 0.05$). SA – salicylic acid, JA – jasmonic acid, OPDA –12-oxophytodienoic acid, ABA – abscisic acid, IAA – indole-3-acetic acid. (**C**) sRNA - GA network is diminished in NahG-Désirée 3 days post PVY^{NTN} inoculation.

Such interconnectedness between plant defense related miRNA/phasiRNA signaling and GA signaling has not been previously identified and may represent a link between defensive and developmental signaling. Thus, we decided to evaluate functionally these results by measuring the concentrations of a set of plant hormones. As predicted by the sRNA-target transcript analyses, we detected a reduced level of GA_3 in PVY^{NTN} infected Désirée plants (**Fig 4B**). The levels of SA, jasmonic acid (JA), the JA precursor 12-oxophytodienoic acid (OPDA), abscisic acid (ABA) and indole-3-acetic acid (IAA) remained unchanged at 3 dpi (**Fig 4B, S9 Dataset**). To inspect if GA deficiency has any impact on plant growth, plants height was monitored till 21 dpi. No differences were observed between all four studied groups of plants.

The miRNA regulatory network and transcriptional regulation are tightly interconnected

Given the critical role of miRNAs in gene regulation, *cis*-regulatory elements of differentially expressed *MIR* genes involved in *R*-gene regulation and GA signaling were investigated. Interestingly, GAMYB binding sites were detected in the promoters of the *MIR6022* and *MIR482f* genes (**S10 Dataset**). Moreover, these genes harbor WRKY8/28/48 binding sites, while *MIR319a* harbors a general WRKY binding W-box regulatory element. Additionally, *cis*-acting elements involved in SA and JA responsiveness were identified in the promoters of the *MIR482f* gene. In all three analyzed promoter sequences for NAC transcription factor binding sites, potentially implicated in defense signaling, were detected (**S10 Dataset**). The promoter of *MIR167e* is only partially assembled in the current version of the potato genome; thus, the promoter analysis was performed only for the first 80 nt upstream of the predicted hairpin precursor sequence (**S10 Dataset**).

sRNA response is attenuated in susceptible SA depleted plants following PVY^{NTN} infection

As the link between repression of GA signaling and disease symptoms severity was already established in Arabidopsis [38] we have further investigated whether the activity of discovered sRNA - GA circuit is acting similarly in susceptible potato – PVY^{NTN} interaction. To keep the same genetic background we have used a transgenic counterpart of Désirée that is depleted in SA accumulation, NahG-Désirée. We have shown previously that in NahG-Désirée plants the pronounced disease symptoms appeared both

on the inoculated and systemic leaves [5]. Furthermore, the viral multiplication was detected 1 day earlier than in non-transgenic Désirée plants (at 4 dpi), while the final concentrations of the virus were not significantly higher [5]. Here, we performed the analysis of sRNA response as well as the measurements of hormonal concentrations in interaction of this susceptible genotype with the virus. Interestingly, we found that the overall response of sRNAs was attenuated in NahG-Désirée at 3 dpi. In NahG-Désirée only 20 miRNAs were differentially expressed, with the majority showing a lower degree of induction than in Désirée plants (**Figs 1 and 2, S1 Dataset**).

Inspecting specifically the discovered link between sRNAs regulation, GA signaling and immune signaling in the sRNA and transcriptional datasets we observed that the responses of miR167e and miR319a are diminished in NahG-Désirée plants (**S1 Dataset**). Interestingly, although the phasiRNA931 was also upregulated in NahG-Désirée plants, albeit to a lower extent, this was not translated into downregulation at the target transcript level (**Fig 4C**). Adding to the significance of this finding, in NahG-Désirée plants the level of bioactive GA was not significantly different in infected leaves (**Fig 4B**). We also compared sRNA-mediated responses in susceptible NahG-Désirée with those observed in tolerant plants of Désirée, which resembled responses in establishment of mutualistic symbioses. Upregulated miR482e targeting NBS-LRR transcripts was observed in both genotypes indicating that this response is not relevant for symptoms development nor is SA-dependent. On the other hand, the relieved silencing of LRR-RLKs by miR6022 that is predicted to potentiate the defence responses and which is also linked with GAMYBs, being involved in symptoms development, was however absent in NahG-Désirée plants (**S4B Fig**). Similarly, the responses of other miRNAs involved in mutualistic symbiosis, such as miR164, miR167, miR171, miR319, miR390, miR393, miR397, miR398, were diminished in NahG plants (**S1 Dataset**).

To evaluate the direct effect of the SA deficiency in NahG plants, independently of the viral infection, we also compared the sRNA expression profiles in mock-inoculated leaves of non-transgenic and SA-depleted Désirée (**Fig 1**). We found 37 miRNAs regulated by SA. It seems that SA in the normal growing conditions generally causes the reduction in the level of miRNAs as majority (28) of miRNAs were detected at significantly higher levels in NahG-Désirée plants (**S1 Dataset**). When we similarly compared the expression profile of transcripts between the two genotypes, we detected that the most strongly induced by SA signaling are notably different WRKY transcription factors (**Table 1, S11 and S12 Datasets**), among them orthologues of Arabidopsis *WRKY70,* which was already shown to be positively regulated by SA [39]. As miR319a and miR482f promotors are regulated by WRKY transcription factors, we discovered a direct link between SA signaling and miRNA regulatory network in potato.

Table 1. SA-dependent transcriptional responses of potato leaves in cv. Désirée.

Functional group (BIN ID)	No. of genes in BIN	NahG-Désirée vs. Désirée
WRKY transcription factor family (27.3.32)	215	-
Biotic stress related regulation of transcription (20.1.5)	140	-
Pathogenesis-related proteins PR-4,8,11 (chitinases and chitin binding proteins) (20.1.7.3)	46	-
Photosynthesis LHC-II (1.1.1.1)	87	-
Glycolysis PEPC (4.3.15)	28	-
Degradation of histidine (13.2.7)	25	-

Gene set enrichment of differences in expression profile was performed comparing mock-inoculated samples of both genotypes and comparing PVY-infected samples of both genotypes using MapMan ontology. Only the gene groups (BINs) significantly enriched (FDR $p < 0.01$) in both comparisons (regulated only by SA and not by the virus) are listed. The full list of enriched BINs is given in **S12 Dataset**. "-" – downregulation of genes assigned to particular BIN was observed in SA deficient plants. No. of genes in BIN – number of all genes assigned to the BIN.

Discussion

We hypothesized that fine-tuned regulation of subsets of genes involved in defensive signaling can interfere with developmental signaling, which could explain decreased symptom severity in plants expressing tolerance to virus infection. The sRNA's have proven to be an important level for precise regulation of several developmental processes. We here show that the integration of sRNA network and transcriptional regulation is also crucial in entanglement of stress responses and developmental processes.

Integration of the sRNA regulatory network with sRNA expression and expression profiles of their targets confirmed many known, but also revealed several novel regulatory circuits associated with immunity regulation and hormone signaling (**Figs 3 and 4, S3 and S4 Figs, S5 and S6 Datasets).** When plants are exposed to pathogens, NBS-LRRs and LRR-RLKs are the key players in sensing and transducing stress signals [40]. Viral suppressors of silencing can release the tight control of *R*-gene silencing by sRNAs and activate immune responses in plants [20,21]. Our study investigated regulatory processes occurring early after infection, before virus concentration significantly increased thus the effects we detected were not caused by extensive HC-Pro or any other viral protein accumulation. Even so, we have detected diverse regulation of NBS-LRRs and LRR-RLKs and their targeting miRNAs as expected according to their specialized roles (**S4 Fig**). Upregulation of miR482e (**S1 Dataset**) and resulting downregulation of its *NBS-LRR* target transcript was shown to enhance the sensitivity of potato to *Verticillium dahliae* infection [27]. On the other hand, upregulation of miR482e was also observed to promote soybean nodulation [28] and could in our system also be part of the network allowing the establishment of commensalistic symbiosis (in plant-virus interaction termed tolerance) between potato

and PVY. Similarity of response between mutualistic symbiosis in soybean and tolerance in potato was also shown by the profile of several other miRNAs (**S1 Dataset**; [29–32]). This suggests a similar modulation of immune response and physiology occurs in both mutualistic and disease tolerant (commensalistic) interactions. In tolerance, plants may adopt some processes resembling mutualistic symbiosis to control plant response and minimize severe disease symptoms allowing non-hindered development of the plant and at the same time multiplication of the virus.

Phytohormones modulate plant defense responses against various biotic and abiotic stresses as well as plant growth and development [41]. Till now, several miRNAs were confirmed to participate in this complex network, mainly in connection to repression of auxin signaling [19]. A similarly complex miR393/miR396/phasiTIR auxin signaling network was identified in this study, yet showing links also to other hormonal signaling pathways (**Fig 3, S3 Fig**).

Most notable is, however, the novel link between sRNA regulatory network and GA signaling. Biotic stress was shown to repress GA signaling pathways [42]. Here, we show that GA biosynthesis and signaling are post-transcriptionally regulated via multiple miRNAs, phasiRNAs as well as vsiRNAs in potato leaves following infection with PVY^{NTN} (**Fig 4A**). The effect of this regulatory circuit was confirmed by reduced bioactive GA level in the tolerant Désirée plants (**Fig 4B**). This reduction was however not reflected in decreased plant growth and was thus most probably transient and localized in nature. sRNAs were shown to regulate GA biosynthesis in potato leaves following PVY^{NTN} infection in three crucial steps, the first step after branching point of GA biosynthesis and the general carotenoid pathway and the last two steps in production of bioactive GA (**Fig 4A**). In other plant species, GA biosynthesis was shown to be indirectly targeted by miRNAs regulating the activity of the corresponding transcription factors (miR319-TCP14-GA2ox/GA20ox; miR393-GRF2-GA3ox/GA20ox) [25], while direct interactions were to our knowledge not yet reported. Also of note, the sRNAs regulating GA biosynthesis identified here were not identified in Arabidopsis and seem to be *Solanaceae* specific.

Moreover, downstream GA signaling components are affected by the sRNA regulatory network as well. *StMYB33*, an orthologue of Arabidopsis GA-induced MYB-like proteins (GAMYBs) *MYB33*, is regulated by miR319a, a close relative of miR159 [43]. The two Arabidopsis *GAMYBs* were shown to be regulated by miR159 [44]. The functional relation between lower activity of GA signaling was already directly confirmed to be related to disease severity in three different experimental systems. Arabidopsis GAMYB double knockout showed ameliorated symptoms when infected with *Cucumber mosaic virus* (CMV) [38], similarly was shown in rice in interaction with bacteria (*Xanthomonas oryzae* pv. *oyrzae*) and fungi (*Magnaporthe oryzae*) using knockout in GA deactivating enzyme [45]. Also in line with this, increase in DELLA protein concentrations was shown to trigger components

of rhizobial and mycorrhizal signaling [46,47], showing yet another similarity between tolerant response of potato to viral infection and response of plants in mutualistic symbiosis.

With the discovery of GAMYB binding sites in the *MIR482f* and *MIR6022* promoters (**S10 Dataset**), we found the circuit in sRNA-GA signaling and additionally a link between GA signaling and *R*-gene expression. The complexity of regulatory responses observed in this study (**Fig 5**) is in line with the systems biology paradigm that interaction of multiple components and not a single component within a cell leads to much of biological function [48]. Although the reductionist approach is powerful in building logically simple hypotheses and devising ways to test them, it is very difficult to reconstitute the function for a whole biological system based solely on that as the behavior of the system may depend heavily on complex interactions within the system [49]. Thus, we have adopted a systems level confirmation of our hypothesis that sRNA-GA-immune signaling circuit is important for establishment of tolerant interaction. Previously, we had demonstrated that SA regulates plant responses to virus infection; not only by delaying viral multiplication, but also by controlling disease symptom severity, most probably via its effects on host primary metabolism [5]. In this study we have confirmed that response of sRNA regulatory networks controlling potential immune receptors and hormonal signaling is strongly attenuated in the NahG-transgenic plants in the early stage of viral infection (3 dpi; **Figs 1 and 2)** showing the role of sRNAs in linking immune signaling and defense. The molecular mechanisms of the link between SA signaling and sRNA network are also complex. SA has been shown to induce *RNA-dependent RNA polymerase 1* expression, which is crucial for the maintenance of basal resistance to several RNA viruses [50,51] but none of the silencing mechanism related enzymes are regulated in SA deficient NahG-Désirée plants (**S11 Dataset;** [7]). We have here predicted SA-directed transcriptional regulation of *MIR482f,* the miRNA linking the GA signaling circuit and *R*-gene expression (**Fig 5, S10 Dataset)**, which could be additional link between SA signaling and symptoms development in potato-PVY interaction. Regulation of miR482f expression by SA was indeed experimentally confirmed in comparison between non-transgenic and NahG-transgenic plants (**S1 Dataset**). An additional link are the WRKY transcription factors that are under positive control of SA (**Table 1**, **S11 and S12 Datasets**) and were predicted to regulate promotors of all three miRNAs involved in sRNA - GA circuit (**Fig 5**).

The outcome of plant-pathogen interactions depends on the delicate balance between plant immune signaling network and its interaction with pathogen. Here, we focused on the roles of sRNA networks in establishment of the tolerance to PVY infection. We showed that the sRNA regulatory network links immune and developmental signaling in potato through newly discovered sRNA - GA circuit. Tolerance of potato to virus infection perturbs sRNA network resulting in downregulation of GA-mediated signaling, as well as modulation of *R*-gene transcript levels; this results in amelioration of disease symptoms. Supporting this, the responses observed for individual miRNAs, *R*-genes and GA-mediated

signaling bear a striking similarity to effects seen during mutualistic symbioses. Modulation of disease severity through GA-mediated signaling was also observed in Arabidopsis infected with mild and severe strains of CMV virus. It is thus plausible that a similar modulation of plant responses occurs in both mutualistic symbiosis and tolerance. This is in line with growing evidence showing that viruses, like other symbionts, lie on a continuum between antagonistic and mutualistic relationships [52,53].

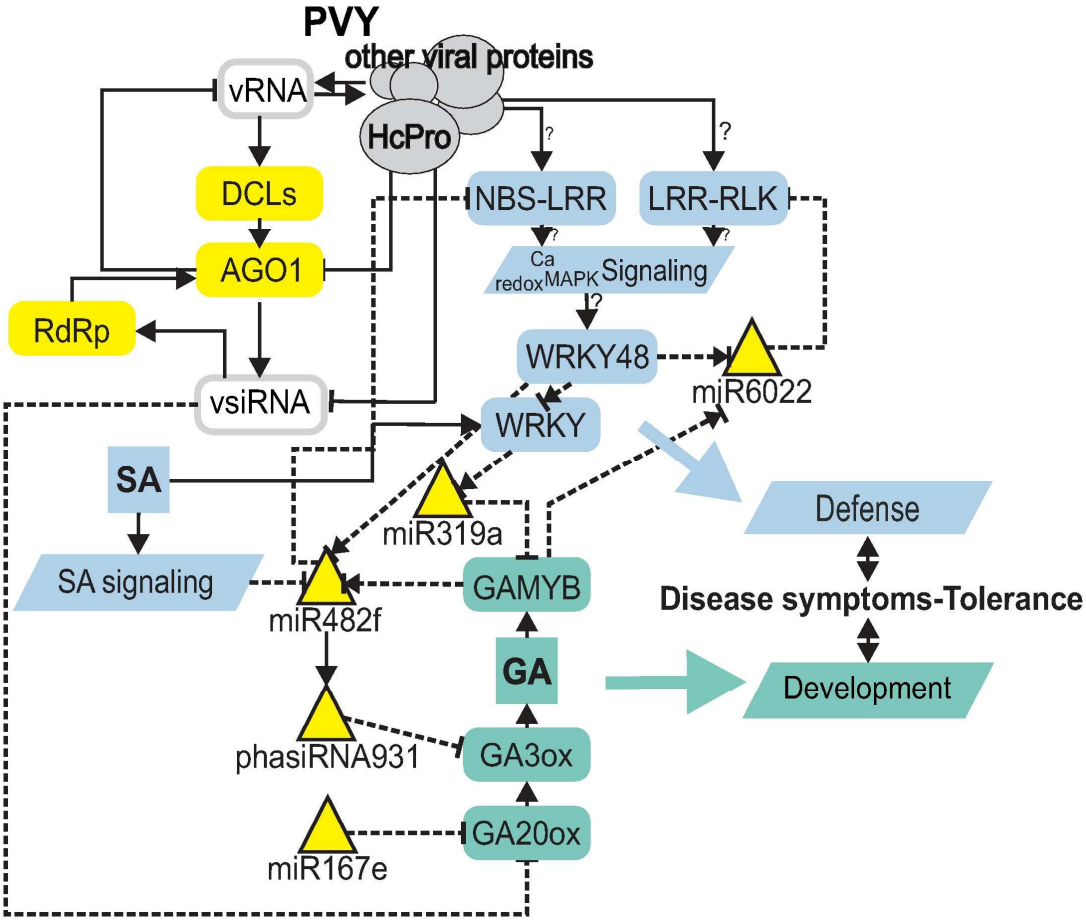

Fig 5. sRNA regulatory network is intertwined with immunity- and gibberellin (GA)-related signaling mediating trade-offs in development and defense. Node color denotes component type/function (grey – virus-derived; yellow – RNA silencing; blue – immune response; green – plant development). Lines represent different types of interaction (solid line – protein level; dashed – transcriptional/post-transcriptional level). Normal arrow – activation, blunt-end arrow – inhibition, combination of normal arrow and blunt-end arrow – unknown mechanism of action. ? – inferred from experiments performed in other species. vRNA – viral RNA; vsiRNA – virus-derived siRNA; HcPro – helper component-proteinase; DCL – DICER-like protein; AGO1 – Argonaute 1; RdRp – RNA-dependent RNA polymerase; NBS-LRR – nucleotide binding site-leucine-rich repeat protein; LRR-RLK – leucine-rich repeat receptor-like kinase; Ca – calcium; MAPK – mitogen activated protein kinase; SA – salicylic acid; GAMYB – GA-induced MYB-like protein; GA – gibberellin; GA20ox – GA20-oxidase; GA3ox – GA3-oxidase.

Materials and methods

Plant material

Potato leaves of cv. Désirée were mock or PVY^{NTN}-inoculated (isolate NIB-NTN, GenBank accession no. AJ585342) as described previously [7]. Plant material of the inoculated leaves was collected 3 days post inoculation (dpi, corresponding to early stages of viral multiplication in both genotypes and before symptoms development in NahG-Désirée plants) for each treatment. Three and four biological replicates (individual leaves from different plants per group) were analyzed for RNA analysis and for hormonal measurements, respectively. Three plants from each group were monitored for plant height, till 21 dpi, when they all started to senesce. The same experimental set up was designed also for analysis of transgenic NahG-Désirée plants [54].

RNA extraction, library preparation and sRNA sequencing

Total RNA was extracted from 100 mg of homogenized leaf tissue using TRIzol reagent (Thermo Fisher Scientific, Waltham, MA) and MaXtract High Density tubes (Qiagen, Hilden, Germany) following manufacturers' protocols. RNA concentration, quality and purity were assessed using agarose gel electrophoresis and NanoDrop ND-1000 spectrophotometer (Thermo Scientific). sRNA NGS libraries were generated from total RNA samples using the TailorMix miRNA Sample Preparation Kit (SeqMatic LLC, Fremont, CA) and sequenced on the Illumina HiSeq 2000 Sequencing System at SeqMatic LLC.

Identification of endogenous and virus-derived sRNAs

The raw reads were quality filtered using Filter Tool of the UEA sRNA Toolkit [55] by discarding low complexity reads (containing at most two distinct nucleotides), reads shorter than 18 nt and longer than 25 nt, reads matching tRNA/rRNA sequences and reads not mapped to the potato genome (PGSC_DM_v4.3) [56]. To identify known annotated miRNAs, the remaining reads were compared to all plant miRNAs registered in miRBase database (release 21) [57], allowing no mismatches. The sequences that matched mature miRNAs from other plants than potato (miRNA orthologs), were mapped to the potato genome to find corresponding *MIR* loci able to form hairpin structure [58] and named according to annotation of conserved miRNA [59]. miRNAs that had different 5′ and 3′ ends with respect to the mature miRNA, were annotated as isomiRs. To identify novel unannotated miRNAs, filtered reads were submitted to miRCat tool of the UEA sRNA Toolkit using default parameters for plants, considering only reads of lengths 18-24 nt. Reads were first mapped to the potato genome, then the 100 and 200 nt long windows around the aligned reads were extracted [58]. The predicted secondary structures were trimmed and analyzed to verify the characteristic hairpin pre-miRNA structure according to plant miRNAs annotation criteria [59]. An additional criterion we have imposed was that novel

miRNAs should be present at least in two analyzed samples with more than five raw reads. Potential novel miRNAs were mapped against miRBase and sequences that matched known plant miRNAs with up to three mismatches were excluded. The novelty of potato specific miRNAs was verified with the miRPlant version 5 [58] using default parameters and additionally rechecked against the latest releases of Rfam [60]; http://rfam.xfam.org/), tRNA [61]; http://gtrnadb.ucsc.edu/) and snoRNA databases [62]; http://snoopy.med.miyazaki-u.ac.jp/). Families of novel miRNAs were determined by clustering their sequences with sequences of known miRNAs using CD-HIT with identity threshold of 0.9 [63]. To identify vsiRNAs, reads of lengths 20-24 nt from all PVY^{NTN}-infected samples were mapped to the reconstructed consensus PVY^{NTN} genome [64] using CLC Genomics Workbench version 8 (http://www.clcbio.com/) allowing only 100 % identity.

Prediction of novel potato phasiRNAs and *PHAS* loci

Prediction of phasiRNAs and phasiRNA-producing loci (*PHAS* loci) was performed using ta-siRNA prediction tool [65] utilizing the potato genome [56] and the merged potato gene and unigene sequences StNIB_v1 [66]. To detect *PHAS* loci with a significant degree of phasing ($p < 0.0001$) and to investigate whether phasing also occurs in sRNAs with phase sizes different from 21 nt, different phasing intervals ranging from 21 to 24 nt were analyzed.

sRNA quantification and statistical analysis

Differential expression analysis was performed in R (R development Core Team, 2011; version 3.2.2), using the limma package [67]. In short, sRNA counts with a baseline expression level of at least two RPM (reads per million of mapped reads) in at least three samples were TMM-normalized (edgeR package, [68]) and log-transformed using voom function [69]. To identify differentially expressed sRNAs the empirical Bayes approach was used and the resultant p-values were adjusted using Benjamini and Hochberg's (FDR) method. Adjusted p-values below 0.05 were considered statistically significant.

Stem-loop RT-qPCR

Stem-loop RT-qPCR was used to quantify the expression of six target miRNAs in relation to the endogenous control (stu-mir167a-5p.1), which was determined to be the most robustly expressed in a sRNA sequencing dataset of potato plants that were uninfected or infected with a range of viruses (PVY, PLRV, PVS, PVX, PVT) (SRA accession no. SRP083247). TaqMan MicroRNA Assays (Thermo Fisher Scientific) were ordered according to the sRNA-Seq sequence of the selected miRNAs (**S2 Table**). Total RNA (1 µg) of the same samples as used for sRNA-Seq was DNase I (Qiagen) treated and reverse transcribed using SuperScript III First-Strand Synthesis System (Thermo Fisher Scientific) and stem-loop Megaplex primer pool (Thermo Fisher Scientific) following the manufacturer's protocol and previously optimized cycling parameters [70]. No template control RT reactions were set to assess

potential Megaplex primer pool background. qPCR reactions were performed in 10 µl volume on the LightCycler480 (Roche Diagnostics Ltd., Rotkreuz, Switzerland) in duplicates and two dilutions (8- and 80-fold) per sample using TaqMan Universal Master Mix II, no UNG (Thermo Fisher Scientific) and TaqMan MicroRNA Assays following the manufacturers' protocols. Additionally, for each miRNA assay, a standard curve was constructed from a serial dilution of the pool of all samples. Raw Cq values were calculated using the second derivative maximum method (Roche Diagnostics Ltd.) and miRNA expression was quantified using a relative standard curve method by normalization to the endogenous control [5]. The statistical significance was assessed by Student's t-test.

sRNA target prediction

In silico identification of potato transcripts targeted by identified sRNAs was carried out using the psRNATarget ([71]; http://plantgrn.noble.org/psRNATarget/) and StNIB_v1 sequences [66], following previously described parameters [72]. Moreover, targets of identified sRNAs were experimentally validated with parallel analysis of RNA ends (PARE) Degradome-Seq. The four degradome libraries (mock Désirée, PVY Désirée, mock NahG-Désirée, PVY NahG-Désirée) were constructed by pooling RNA of the biological replicates and sequenced on the Illumina HiSeq 2500 platform. The data were analyzed at LC Sciences (Houston, TX) with CleaveLand4 ([73]; http://sites.psu.edu/axtell/software/cleaveland4/) using all our experimentally identified sRNAs and the StNIB_v1 sequences allowing for maximum three mismatches. All identified degradation targets were classified into 5 categories as previously described [73]. Only categories 0-3 with high cleavage signal were considered as reliable cleavage. Results of miRNA-target (*PHAS* loci) interactions were also used to reveal miRNA triggers of the phasiRNA production. Only 22-nt miRNAs were kept as potential triggers [15,16].

Regulatory network construction

In order to compare the expression of sRNAs with the expression of their target transcripts we used a microarray gene expression dataset generated from the same samples ([7]; GEO accession no. GSE58593). All differentially expressed miRNAs and phasiRNAs were analyzed for functional overrepresentation in biological pathways with MapMan software [74] using the ontology adapted for potato [66,75]. All sRNAs and their targets, obtained by *in silico* prediction and Degradome-Seq were integrated with their expression data and used for construction of regulatory networks in Cytoscape 3.4 [76].

Identification of *cis*-regulatory elements in promoter regions of *MIR* genes

1000 nt sequences upstream of the predicted *MIR* gene hairpin sequences were extracted as putative miRNA promoter regions [77] and scanned for *cis*-regulatory elements of plant transcription factors using position weight matrices and transcription binding sites in TRANSFAC [78]; http://www.biobase-international.com/product/transcription-factor-binding-sites) and PlantCARE [79]; http://bioinformatics.psb.ugent.be/webtools/plantcare/html/) databases.

Hormonal measurements

Hormone contents were determined by gas chromatography coupled with mass spectrometry (GC-MS). Approximately 100 mg of plant material was collected for each sample and 1 ml of 100% methanol (HPLC grade) was added. The following stable isotope-labeled compounds were added as internal standards to each sample prior to the extraction: 50 pmol [$^2H_4$]-SA, 50 pmol [$^2H_5$]-JA, 50 pmol [$^2H_2$]-IAA, 50 pmol [$^2H_2$]-GA A_3, 33 pmol [$^2H_6$]-ABA, 15 pmol [$^2H_5$]-OPDA. Next, the samples were heated at 60 °C for 5 min and then incubated at room temperature for 1 h with occasional vortexing. The methanolic phase was taken to complete dryness *in vacuo*. The resulting residue was dissolved in methanol (50 µl) to which diethyl ether (200 µl) was added. The samples were sonified (5 min) and centrifuged (5 min, 14,000 *g*). The particle-free supernatant was loaded to aminopropyl solid-phase extraction cartridges (Chromabond NH_2 shorty 10 mg; Macherey–Nagel GmbH, Düren, Germany). Each cartridge was washed twice with $CHCl_3$:2-propanol (2:1, v/v, 250 µl) before the hormone containing fraction was eluted with acidified diethyl ether (2 % acetic acid, v/v, 400 µl). The eluates were transferred into 0.8 ml autosampler vials and again taken to dryness in a gentle stream of nitrogen. Prior to MS assessment, the samples were derivatized with a 20 µl of a mix of acetone:methanol (9:1, v/v, 220 µl), diethyl ether (27 µl) and (trimethylsilyl)diazomethane solution (2.0 M in diethyl ether, 3 µl) and letting them rest for 30 min at room temperature. The setting for the GC and the MS were as described previously [80]. For the determination of endogenous and stable isotope-labeled methylated acidic plant hormones, respectively, the following ion transitions were recorded: MeSA m/z 152 to m/z 120 and m/z 156 to m/z 124 for [$^2H_4$]-MeSA, retention time 6.75 ± 0.4 min; MeOPDA m/z 238 to m/z 163 and m/z 243 to m/z 168 for [$^2H_5$]-MeOPDA, retention time 10.00 ± 0.4 min; MeJA m/z 224 to m/z 151 and m/z 229 to m/z 154 for [$^2H_5$]-MeJA, retention time 11.27 ± 0.5 min; MeIAA m/z 189 to m/z 130 and m/z 191 to m/z 132 for [$^2H_2$]-MeIAA, retention time 13.34 ± 0.4 min; MeABA m/z 162 to m/z 133 and m/z 168 to m/z 139 for [$^2H_6$]-MeABA, retention time 15.78 ± 0.4 min; and MeGA m/z 136 to m/z 120 and m/z 138 to m/z 122 for [$^2H_2$]-MeGA, retention time 21.67 ± 0.6 min. The amounts of endogenous hormone contents were calculated from the signal ratio of the unlabeled over the stable isotope-containing mass fragment observed in the parallel measurements. Significant changes in hormone concentrations between treatment-genotype groups were determined by ANOVA followed by

LSD post hoc analysis (Benjamini Hochberg FDR p-value adjustment, alpha= 0.05) using the Agricolae R package.

Gene set enrichment analysis

To identify SA regulated genes in cv. Désirée the normalized expression values between mock NahG-Désirée vs. Désirée and PVY-infected NahG-Désirée vs. Désirée samples were compared (calculated from the 3 dpi samples; data of Stare et al. [7]. Gene Set Enrichment Analysis (GSEA; [81] was performed (false discovery rate corrected q $\leq$0.01) comparing expression profiles between both genotypes, using MapMan ontology as the source of the gene sets.

Data deposition and Gene IDs

The sRNA and Degradome-Seq data can be accessed at the NCBI's Gene expression omnibus (GEO) under accession numbers GSE84851 and GSE84967. Full list of gene/protein names used in this manuscript, together with their Gene IDs, short names, Arabidopsis orthologue genes is given in **S1 Table**.

Acknowledgments

The authors would like to acknowledge dr. Tjaša Stare for providing plant material, dr. Sabine Rosahl for providing NahG-Désirée potato plants. Katja Stare and Tjaša Lukan for technical support, Maja Zagorščak for providing the script to determine the location of *MIR* loci in the potato genome, dr.Denis Kutnjak for the help with PVY^{NTN} genome assembly and dr. John Carr and dr. Anna Coll Rius for critical reading of the manuscript and fruitful discussions.

References

[1] Solomon-Blackburn RM, Barker H. Breeding virus resistant potatoes (Solanum tuberosum): A review of traditional and molecular approaches. Heredity (Edinb) 2001;86:17–35. doi:10.1046/j.1365-2540.2001.00799.x.

[2] Karasev A V, Gray SM. Continuous and emerging challenges of Potato virus Y in potato. Annu Rev Phytopathol 2013;51:571–86. doi:10.1146/annurev-phyto-082712-102332.

[3] Scholthof KBG, Adkins S, Czosnek H, Palukaitis P, Jacquot E, Hohn T, et al. Top 10 plant viruses in molecular plant pathology. Mol Plant Pathol 2011;12:938–54. doi:10.1111/j.1364-3703.2011.00752.x.

[4] Ravnikar M. Physiology of the Potato – Potato Virus Y Interaction 2013:1–31. doi:10.1007/978-3-642-30967-0.

[5] Baebler Š, Stare K, Kovač M, Blejec A, Prezelj N, Stare T, et al. Dynamics of responses in compatible

potato - potato virus y interaction are modulated by salicylic acid. PLoS One 2011;6. doi:10.1371/journal.pone.0029009.

[6] Wilson C. Management of Virus Disease: Host Resistance. Wallingford, Oxfordshire, UK CABI; 2014.

[7] Stare T, Ramšak Ž, Blejec A, Stare K, Turnšek N, Weckwerth W, et al. Bimodal dynamics of primary metabolism-related responses in tolerant potato-Potato virus Y interaction. BMC Genomics 2015;16:716. doi:10.1186/s12864-015-1925-2.

[8] Baulcombe D. RNA silencing in plants. Nature 2004;431:356–63. doi:10.1038/nature02874.

[9] Csorba T, Kontra L, Burgyán J. Viral silencing suppressors: Tools forged to fine-tune host-pathogen coexistence. Virology 2015;479–480:85–103. doi:10.1016/j.virol.2015.02.028.

[10] Ivanov KI, Eskelin K, Bašic M, De S, Lõhmus A, Varjosalo M, et al. Molecular insights into the function of the viral RNA silencing suppressor HCPro. Plant J 2016;85:30–45. doi:10.1111/tpj.13088.

[11] Zvereva AS, Pooggin MM. Silencing and innate immunity in plant defense against viral and non-viral pathogens. Viruses 2012;4:2578–97. doi:10.3390/v4112578.

[12] Singh RP, Valkonen JPT, Gray SM, Boonham N, Jones RAC, Kerlan C, et al. Discussion paper: The naming of Potato virus Y strains infecting potato. Arch Virol 2008;153:1–13. doi:10.1007/s00705-007-1059-1.

[13] Seo J-K, Wu J, Lii Y, Li Y, Jin H. Contribution of small RNA pathway components in plant immunity. Mol Plant Microbe Interact 2013;26:617–25. doi:10.1094/MPMI-10-12-0255-IA.

[14] Meng Y, Shao C, Wang H, Chen M. The Regulatory Activities of Plant MicroRNAs: A More Dynamic Perspective. Plant Physiol 2011;157:1583–95. doi:10.1104/pp.111.187088.

[15] Chen H-M, Chen L-T, Patel K, Li Y-H, Baulcombe DC, Wu S-H. 22-Nucleotide RNAs trigger secondary siRNA biogenesis in plants. Proc Natl Acad Sci U S A 2010. doi:10.1073/pnas.1001738107.

[16] Cuperus JT, Carbonell A, Fahlgren N, Garcia-Ruiz H, Burke RT, Takeda A, et al. Unique functionality of 22-nt miRNAs in triggering RDR6-dependent siRNA biogenesis from target transcripts in Arabidopsis. Nat Struct Mol Biol 2010;17:997–1003. doi:10.1038/nsmb.1866.

[17] Borges F, Martienssen RA. The expanding world of small RNAs in plants. Nat Publ Gr 2015;16:1–15. doi:10.1038/nrm4085.

[18] Peláez P, Sanchez F. Small RNAs in plant defense responses during viral and bacterial interactions: similarities and differences. Front Plant Sci 2013;4:343. doi:10.3389/fpls.2013.00343.

[19] Navarro L, Dunoyer P, Jay F, Arnold B, Dharmasiri N, Estelle M, et al. Repressing Auxin Signaling. Science (80-) 2005.

[20] Li F, Pignatta D, Bendix C, Brunkard JO, Cohn MM, Tung J, et al. MicroRNA regulation of plant innate immune receptors. Proc Natl Acad Sci U S A 2011;109:1790–5. doi:10.1073/pnas.1118282109/-/DCSupplemental.www.pnas.org/cgi/doi/10.1073/pnas.1118282109.

[21] Shivaprasad P V., Chen H-M, Patel K, Bond DM, Santos B a. CM, Baulcombe DC. A MicroRNA Superfamily Regulates Nucleotide Binding Site-Leucine-Rich Repeats and Other mRNAs. Plant Cell 2012;24:859–74. doi:10.1105/tpc.111.095380.

[22] Park JH, Shin C. The role of plant small RNAs in NB-LRR regulation. Brief Funct Genomics 2015:1–7. doi:10.1093/bfgp/elv006.

[23] Axtell MJ, Jan C, Rajagopalan R, Bartel DP. A Two-Hit Trigger for siRNA Biogenesis in Plants. Cell 2006;127:565–77. doi:10.1016/j.cell.2006.09.032.

[24] Finn RD, Coggill P, Eberhardt RY, Eddy SR, Mistry J, Mitchell AL, et al. The Pfam protein families database : towards a more sustainable future 2016;44:279–85. doi:10.1093/nar/gkv1344.

[25] Curaba J, Singh MB, Bhalla PL. MiRNAs in the crosstalk between phytohormone signalling pathways. J Exp Bot 2014;65:1425–38. doi:10.1093/jxb/eru002.

[26] Ouyang S, Park G, Atamian HS, Han CS, Stajich JE, Kaloshian I, et al. MicroRNAs Suppress NB

Domain Genes in Tomato That Confer Resistance to Fusarium oxysporum. PLoS Pathog 2014;10. doi:10.1371/journal.ppat.1004464.

[27] Yang L, Mu X, Liu C, Cai J, Shi K, Zhu W, et al. Overexpression of potato miR482e enhanced plant sensitivity to Verticillium dahliae infection. J Integr Plant Biol 2015;57:1078–88. doi:10.1111/jipb.12348.

[28] Li H, Deng Y, Wu TL, Subramanian S, Yu O. Misexpression of miR482, miR1512, and miR1515 increases soybean nodulation. Plant Physiol 2010;153:1759–70. doi:10.1104/pp.110.156950.

[29] Mao G, Turner M, Yu O, Subramanian S. miR393 and miR164 influence indeterminate but not determinate nodule development. Plant Signal Behav 2013;8:doi: 10.4161/psb.26753. doi:10.4161/psb.26753.

[30] Yan Z, Hossain MS, Arikit S, Vald??s-L??pez O, Zhai J, Wang J, et al. Identification of microRNAs and their mRNA targets during soybean nodule development: Functional analysis of the role of miR393j-3p in soybean nodulation. New Phytol 2015;207:748–59. doi:10.1111/nph.13365.

[31] Lelandais-Brière C, Naya L, Sallet E, Calenge F, Frugier F, Hartmann C, et al. Genome-wide Medicago truncatula small RNA analysis revealed novel microRNAs and isoforms differentially regulated in roots and nodules. Plant Cell 2009;21:2780–96. doi:10.1105/tpc.109.068130.

[32] De Luis A, Markmann K, Cognat V, Holt DB, Charpentier M, Parniske M, et al. Two microRNAs linked to nodule infection and nitrogen-fixing ability in the legume Lotus japonicus. Plant Physiol 2012;160:2137–54. doi:10.1104/pp.112.204883.

[33] Yamaguchi S. Gibberellin Metabolism and its Regulation. Annu Rev Plant Biol 2008;59:225–51. doi:10.1146/annurev.arplant.59.032607.092804.

[34] Griffiths-Jones S, Grocock RJ, van Dongen S, Bateman A, Enright AJ. miRBase: microRNA sequences, targets and gene nomenclature. Nucleic Acids Res 2006;34:D140–4. doi:10.1093/nar/gkj112.

[35] Zhang C, Li G, Zhu S, Zhang S, Fang J. tasiRNAdb: a database of ta-siRNA regulatory pathways. Bioinformatics 2014;30:1045–6. doi:10.1093/bioinformatics/btt746.

[36] Millar AA, Gubler F. The Arabidopsis GAMYB-Like Genes , MYB33 and MYB65 , Are MicroRNA-Regulated Genes That Redundantly Facilitate Anther Development. Plant Cell 2005;17:705–21. doi:10.1105/tpc.104.027920.).

[37] Rogers K, Chen X. Biogenesis, Turnover, and Mode of Action of Plant MicroRNAs. Plant Cell 2013;25:2383–99. doi:10.1105/tpc.113.113159.

[38] Du Z, Chen A, Chen W, Westwood JH, Baulcombe DC, Carr JP. Using a viral vector to reveal the role of microRNA159 in disease symptom induction by a severe strain of Cucumber mosaic virus. Plant Physiol 2014;164:1378–88. doi:10.1104/pp.113.232090.

[39] Li J, Brader G, Palva ET. The WRKY70 Transcription Factor: A Node of Convergence for Jasmonate-Mediated and Salicylate-Mediated Signals in Plant Defense. Plant Cell 2004;16:319–31. doi:10.1105/tpc.016980.

[40] Jones JDG, Dangl JL. The plant immune system. Nature 2006;444:323–9. doi:10.1038/nature05286.

[41] Huot B, Yao J, Montgomery BL, He SY. Growth-defense tradeoffs in plants: A balancing act to optimize fitness. Mol Plant 2014;7:1267–87. doi:10.1093/mp/ssu049.

[42] Wang D, Pajerowska-Mukhtar K, Culler AH, Dong X. Salicylic Acid Inhibits Pathogen Growth in Plants through Repression of the Auxin Signaling Pathway. Curr Biol 2007;17:1784–90. doi:10.1016/j.cub.2007.09.025.

[43] Palatnik JF, Wollmann H, Schommer C, Schwab R, Boisbouvier J, Rodriguez R, et al. Sequence and Expression Differences Underlie Functional Specialization of Arabidopsis MicroRNAs miR159 and miR319. Dev Cell 2007;13:115–25. doi:10.1016/j.devcel.2007.04.012.

[44] Allen RS, Li J, Stahle MI, Dubroué A, Gubler F, Millar AA. Genetic analysis reveals functional redundancy and the major target genes of the Arabidopsis miR159 family. Proc Natl Acad Sci 2007;104:16371–6. doi:10.1073/pnas.0707653104.

[45] Yang DL, Li Q, Deng YW, Lou YG, Wang MY, Zhou GX, et al. Altered disease development in the eui mutants and Eui overexpressors indicates that gibberellins negatively regulate rice basal disease resistance. Mol Plant 2008;1:528–37. doi:10.1093/mp/ssn021.

[46] Jin Y, Liu H, Luo D, Yu N, Dong W, Wang C, et al. DELLA proteins are common components of symbiotic rhizobial and mycorrhizal signalling pathways. Nat Commun 2016;7:12433. doi:10.1038/ncomms12433.

[47] Fonouni-Farde C, Tan S, Baudin M, Brault M, Wen J, Mysore KS, et al. DELLA-mediated gibberellin signalling regulates Nod factor signalling and rhizobial infection. Nat Commun 2016;7:12636. doi:10.1038/ncomms12636.

[48] Westerhoff H V., Nakayama S, Mondeel TDGA, Barberis M. Systems Pharmacology: An opinion on how to turn the impossible into grand challenges. Drug Discov Today Technol 2015;15:23–31. doi:10.1016/j.ddtec.2015.06.006.

[49] Approach T. Perspectives on Systems Biology Attacking Complex Problems with the Power of 2003;132:417–9. doi:10.1104/pp.103.021774.It.

[50] Carr JP, Lewsey MG, Palukaitis P. Signaling in Induced Resistance. Adv. Virus Res., vol. 76, Elsevier Inc.; 2010, p. 57–121. doi:10.1016/S0065-3527(10)76003-6.

[51] Yu D, Fan B, MacFarlane S a, Chen Z. Analysis of the involvement of an inducible Arabidopsis RNA-dependent RNA polymerase in antiviral defense. Mol Plant Microbe Interact 2003;16:206–16. doi:10.1094/MPMI.2003.16.3.206.

[52] Roossinck MJ. Move Over, Bacteria! Viruses Make Their Mark as Mutualistic Microbial Symbionts. J Virol 2015;89:6532–5. doi:10.1128/JVI.02974-14.

[53] Kamitani M, Nagano AJ, Honjo MN, Kudoh H. RNA-Seq reveals virus-virus and virus-plant interactions in nature. FEMS Microbiol Ecol 2016;92:1–11. doi:10.1093/femsec/iw176.

[54] Halim VA, Hunger A, Macioszek V, Landgraf P, Nürnberger T, Scheel D, et al. The oligopeptide elicitor Pep-13 induces salicylic acid-dependent and -independent defense reactions in potato. Physiol Mol Plant Pathol 2004;64:311–8. doi:10.1016/j.pmpp.2004.10.003.

[55] Moxon S, Schwach F, Dalmay T, MacLean D, Studholme DJ, Moulton V. A toolkit for analysing large-scale plant small RNA datasets. Bioinformatics 2008;24:2252–3. doi:10.1093/bioinformatics/btn428.

[56] Xu X, Pan S, Cheng S, Zhang B, Mu D, Ni P, et al. Genome sequence and analysis of the tuber crop potato. Nature 2011;475:189–95. doi:10.1038/nature10158.

[57] Kozomara A, Griffiths-jones S. miRBase : annotating high confidence microRNAs using deep sequencing data 2014;42:68–73. doi:10.1093/nar/gkt1181.

[58] An J, Lai J, Sajjanhar A, Lehman M, Nelson C. miRPlant: an integrated tool for identification of plant miRNA from RNA sequencing data. BMC Bioinformatics 2014;15:275. doi:citeulike-article-id:13323934\rdoi: 10.1186/1471-2105-15-275.

[59] Meyers BC, Axtell MJ, Bartel B, Bartel DP, Baulcombe D, Bowman JL, et al. Criteria for annotation of plant MicroRNAs. Plant Cell 2008;20:3186–90. doi:10.1105/tpc.108.064311.

[60] Nawrocki EP, Burge SW, Bateman A, Daub J, Eberhardt RY, Eddy SR, et al. Rfam 12.0: Updates to the RNA families database. Nucleic Acids Res 2015;43:D130–7. doi:10.1093/nar/gku1063.

[61] Chan PP, Lowe TM. GtRNAdb 2.0: an expanded database of transfer RNA genes identified in complete and draft genomes. Nucleic Acids Res 2016;44:D184-9. doi:10.1093/nar/gkv1309.

[62] Yoshihama M, Nakao A, Kenmochi N. snOPY: a small nucleolar RNA orthological gene database. BMC Res Notes 2013;6:426. doi:10.1186/1756-0500-6-426.

[63] Huang Y, Niu B, Gao Y, Fu L, Li W. CD-HIT Suite: A web server for clustering and comparing biological sequences. Bioinformatics 2010;26:680–2. doi:10.1093/bioinformatics/btq003.

[64] Kutnjak D, Rupar M, Gutierrez-Aguirre I, Curk T, Kreuze JF, Ravnikar M. Deep sequencing of virus derived small interfering RNAs and RNA from viral particles shows highly similar mutational landscape

of a plant virus population. J Virol 2015;89:4760–9. doi:10.1128/JVI.03685-14.

[65] Chen H, Li Y, Wu S. Bioinformatic prediction and experimental validation of a microRNA-directed tandem trans-acting siRNA cascade in Arabidopsis 2007.

[66] Ramšak Ž, Baebler Š, Rotter A, Korbar M, Mozetič I, Usadel B, et al. GoMapMan: Integration, consolidation and visualization of plant gene annotations within the MapMan ontology. Nucleic Acids Res 2014;42:1167–75. doi:10.1093/nar/gkt1056.

[67] Ritchie ME, Phipson B, Wu D, Hu Y, Law CW, Shi W, et al. Limma powers differential expression analyses for RNA-sequencing and microarray studies. Nucleic Acids Res 2015;43:e47. doi:10.1093/nar/gkv007.

[68] Robinson MD, McCarthy DJ, Smyth GK. edgeR: A Bioconductor package for differential expression analysis of digital gene expression data. Bioinformatics 2009;26:139–40. doi:10.1093/bioinformatics/btp616.

[69] Law CW, Chen Y, Shi W, Smyth GK. voom: Precision weights unlock linear model analysis tools for RNA-seq read counts. Genome Biol 2014;15:R29. doi:10.1186/gb-2014-15-2-r29.

[70] Varkonyi-Gasic E, Wu R, Wood M, Walton EF, Hellens RP. Protocol: a highly sensitive RT-PCR method for detection and quantification of microRNAs. Plant Methods 2007;3:12. doi:10.1186/1746-4811-3-12.

[71] Dai X, Zhao PX. PsRNATarget: A plant small RNA target analysis server. Nucleic Acids Res 2011;39:1–5. doi:10.1093/nar/gkr319.

[72] Zhang R, Marshall D, Bryan GJ, Hornyik C. Identification and Characterization of miRNA Transcriptome in Potato by High-Throughput Sequencing. PLoS One 2013;8. doi:10.1371/journal.pone.0057233.

[73] Addo-Quaye C, Miller W, Axtell MJ. CleaveLand: A pipeline for using degradome data to find cleaved small RNA targets. Bioinformatics 2009;25:130–1. doi:10.1093/bioinformatics/btn604.

[74] Usadel B, Poree F, Nagel A, Lohse M, Czedik-Eysenberg A, Stitt M. A guide to using MapMan to visualize and compare Omics data in plants: A case study in the crop species, Maize. Plant, Cell Environ 2009;32:1211–29. doi:10.1111/j.1365-3040.2009.01978.x.

[75] Rotter A, Usadel B, Baebler S, Stitt M, Gruden K. Adaptation of the MapMan ontology to biotic stress responses: application in solanaceous species. Plant Methods 2007;3:10. doi:10.1186/1746-4811-3-10.

[76] Shannon P, Markiel A, Ozier O, Baliga NS, Wang JT, Ramage D, et al. Cytoscape: A software Environment for integrated models of biomolecular interaction networks. Genome Res 2003;13:2498–504. doi:10.1101/gr.1239303.

[77] Megraw M, Hatzigeorgiou AG. MicroRNA Promoter Analysis. In: Walker JM, editor. Plant MicroRNAs, vol. 592, 2010, p. 149–61. doi:10.1007/978-1-60327-005-2.

[78] Matys V, Fricke E, Geffers R, Gößling E, Haubrock M, Hehl R, et al. TRANSFAC®: Transcriptional regulation, from patterns to profiles. Nucleic Acids Res 2003;31:374–8. doi:10.1093/nar/gkg108.

[79] Lescot M, Déhais P, Thijs G, Marchal K, Moreau Y, Van de Peer Y, et al. PlantCARE, a database of plant cis-acting regulatory elements and a portal to tools for in silico analysis of promoter sequences. Nucleic Acids Res 2002;30:325–7. doi:10.1093/nar/30.1.325.

[80] Sanz L, Fernandez-Marcos M, Modrego A, Lewis DR, Muday GK, Pollmann S, et al. Nitric Oxide Plays a Role in Stem Cell Niche Homeostasis through Its Interaction with Auxin(1 W OPEN). Plant Physiol 2014;166:1972-U1195. doi:10.1104/pp.114.247445.

[81] Subramanian A, Tamayo P, Mootha VK, Mukherjee S, Ebert BL, Gillette M a, et al. Gene set enrichment analysis: a knowledge-based approach for interpreting genome-wide expression profiles. Proc Natl Acad Sci U S A 2005;102:15545–50. doi:10.1073/pnas.0506580102.